Global climatic impacts of a collapse of the Atlantic thermohaline circulation.

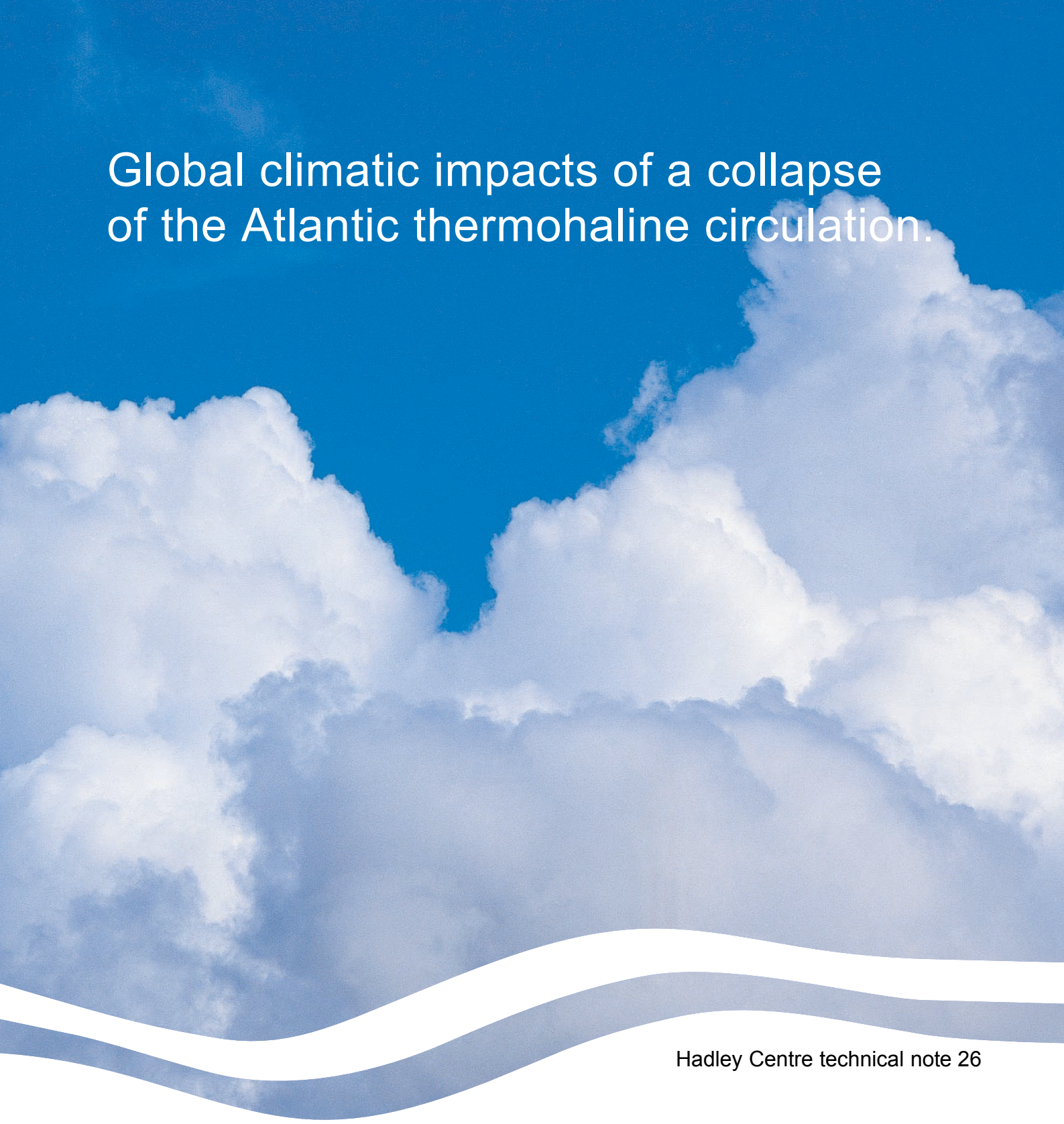

Hadley Centre technical note 26

Michael Vellinga and Richard A. Wood

February 2001

Met Office

Global climatic impacts of a collapse of the Atlantic thermohaline circulation

Michael Vellinga, Richard A. Wood

Met Office, Hadley Centre for Climate Prediction and Research

London Road, Bracknell, Berkshire RG12 2SY, United Kingdom

20 February 2001

Abstract

Part of the uncertainty in predictions by climate models results from limited knowledge of the stability of the thermohaline circulation of the ocean. Here we provide estimates of the response of pre-industrial surface climate variables should the thermohaline circulation in the Atlantic Ocean collapse. For this we have used HadCM3, an ocean-atmosphere general circulation model that is run without flux adjustments. In this model a temporary collapse was forced by applying a strong initial freshening to the top layers of the North Atlantic.

In the first five decades after the collapse surface air temperature response is dominated by cooling of much of the Northern Hemisphere (locally up to 8^oC, $1-2^oC$ on average) and weak warming of the Southern Hemisphere (locally up to 1^oC, 0.2^oC on average). Response is strongest around the North Atlantic but significant changes occur over the entire globe and highlight rapid teleconnections. Drier soil conditions occur over Europe and Asia due to a stronger reduction in precipitation than in evaporation. A southward shift of the Intertropical Convergence Zone over the Atlantic and eastern Pacific creates regionally large changes in precipitation in South America and Africa. Colder and drier conditions in much of the Northern Hemisphere reduce the net primary productivity of the terrestrial vegetation. This is only partly compensated by more productivity in the Southern Hemisphere. The total global net primary production by the vegetation decreases by 5%. After about 100 years the model's thermohaline circulation has largely recovered, and most climatic anomalies disappear.

1 Introduction

A well-known property of present-day climate is the overall northward rather than poleward heat transport in the Atlantic Ocean (e.g Macdonald and Wunsch (1996)). This is a manifestation of the conveyor belt-like structure by which the thermohaline circulation of the ocean ('THC') organises the global heat transport (Gordon (1986)). The deep outflow of cold North Atlantic Deep Water is matched by a warm northward surface flow. This effectively transports heat into the North Atlantic which, when released, moderates climate in northwestern Europe.

Palaeoclimatic records suggest that this mode of ocean circulation is not unique. Different modes are believed to have occurred during glacial times and periods of deglaciation (Sarnthein *et al.* (1994)). For present insolation and ice sheet conditions experiments by Manabe and Stouffer (1988); Manabe and Stouffer (1999) with the GFDL climate model suggest that there may be two possible climate states: one with and one without North Atlantic Deep Water ('NADW') formation, and associated presence or absence of a vigorous THC. In the state without a vigorous THC air temperatures in the Northern Hemisphere were found locally to be up to 9^0C cooler (Manabe and Stouffer (1988)). How likely it is that the THC might collapse in the near future is unclear, as there remains a large uncertainty in modelled stability of the present THC. The two climate equilibria found in the GFDL model have so far not been identified in other climate GCMs (e.g. Schiller *et al.* (1997),Vellinga and Wood (2001)). Furthermore, there is disagreement amongst climate models about the response of the THC to increased greenhouse gas concentrations though none of these predict a THC collapse over the next century (Manabe and Stouffer (1994); Wood *et al.* (1999); Latif *et al.* (2000); Thorpe *et al.* (2001)). Questions about the likelihood of a collapse of the THC in this century are left aside here.

Nevertheless, the question of what the climate response to an eventual collapse would be is an important one, both from physical and socio-economic points of view (Keller *et al.* (2000)). Possible climate response to a THC collapse has been described before by Schiller *et al.* (1997); Manabe and Stouffer (1988) using climate models that require flux adjustments. These are artificial fluxes that prevent the models' control climate from drifting, but do so at the cost of obscuring the model response to a THC collapse (e.g. because they may modify the relationship between meridional heat transport and climate state).

The most recent version of the Hadley Centre climate model (HadCM3) has maintained a stable climate simulation for over 1000 years without the use of flux adjustments (Gordon *et al.* (2000)). It is a global atmosphere

-ocean model with sea ice and land surface schemes. We have used this model to analyse the climate response caused by a forced collapse of the THC. The physical processes in the atmosphere and oceans that result from this event, and that eventually lead to a recovery of the THC are described by Vellinga and Wood (2001). In the current paper we will describe the response in a number of quantities relating to surface climate conditions and where possible compare them to other estimates. To analyse the THC response *per se*, i.e. in isolation from any anthropogenic climate perturbations, we have carried out the experiment for a pre-industrial climate state. It will provide an upper bound for the uncertainty in climate predictions that is caused by any errors in predicting the THC stability. It will also give potential input to impacts models used to study the consequenses of a THC collapse.

A brief description of the model and the set-up of the experiment is given in section 2. The climate response is given in section 3. Conclusions follow in section 4.

2 Model and experimental set-up

The climate model that has been used in this study is HadCM3, a coupled ocean-atmosphere model, with sea-ice and land surface schemes. The atmosphere model has a resolution of $2.5^o \times 3.75^o$, with 19 vertical levels. The ocean model has a resolution of $1.25^o \times 1.25^o$ and has 20 vertical levels. The model maintains a stable surface climate throughout a control run of over 1000 years with fixed pre-industrial greenhouse gas concentrations, without the use of flux correction. Details of the model and a validation of its control climate are given by Gordon *et al.* (2000) and Pope *et al.* (2000). This experiment will be referred to as 'control run' in this paper. The model simulates a realistic ocean heat transport which is relevant to the results presented here. Wood *et al.* (1999) present a validation of the THC in the North Atlantic.

We produced a weakened THC in the model by perturbing the state that the control integration of HadCM3 had reached after 100 years. The top 800m of the North Atlantic ($[80^oW - 20^oE] \times [50^oN - 90^oN]$) were made fresher by about 2 psu. Assuming a reference salinity of 35 psu, the area would have to receive a freshwater pulse of about $6 \cdot 10^{14} m^3 (\approx 20\ Sv * year; 1\ Sv \equiv 10^6 m^3 s^{-1})$ to experience this freshening. Conservation of salt was assured by globally redistributing the salt taken out of the North Atlantic. The model was allowed to adjust freely to the new salinity field in an integration of 150 years, referred to as 'perturbation

run'. We emphasize here that after about 100 years the THC had regained its original strength. Aspects of the adjustment process and climate feedbacks that lead to this recovery are described by Vellinga and Wood (2001). The responses in a number of surface climate variables are given in the next section.

Climate response after the collapse of the THC is measured in terms of anomalies between the perturbation and the control experiments. To extract this signal from the natural variability of the control climate, only anomalies exceeding two standard deviations (of the corresponding meaning period from the control experiment) are deemed significant.

3 Climate response

Within 10 years after the salinity perturbation is applied the Atlantic THC (as measured by the zonally averaged meridional circulation) collapses (Vellinga and Wood (2001)). This eliminates the northward heat transport and associated heat release in the North Atlantic. As mentioned already the model is not in equilibrium during the first 100 years of the experiment. Nevertheless, the transient climate response allows an assessment of the impact that a THC collapse would have. To see if anomalies spread globally we mostly present fields for years 20-30 of the experiment, even though the response around the North Atlantic is sometimes stronger in the first decade.

The sequence of this analysis will be: surface air temperature (sec. 3.1), surface winds (sec. 3.2), precipitation and evaporation (sec. 3.3) and implications for the vegetation (sec. 3.4).

3.1 Surface air temperature

The collapse of the THC causes rapid global change in surface air temperature (Figure1). Within 20 years after the shutdown of the THC persistent anomalies (lasting two or more decades) have covered most of the Northern Hemisphere. In the Southern Hemisphere the response takes longer to become apparent, up to three decades.

The reduction of northward heat transport and surface heat release in the North Atlantic lead to significant cooling of the air in that area. Maximum cooling of up to 8^oC occurs over the northwest Atlantic. Over Europe the cooling is about $2-3^oC$ in the third decade after the THC collapse (Figure 2). The comparatively strong cooling over the northwest Atlantic and Labrador Sea and the Sea of

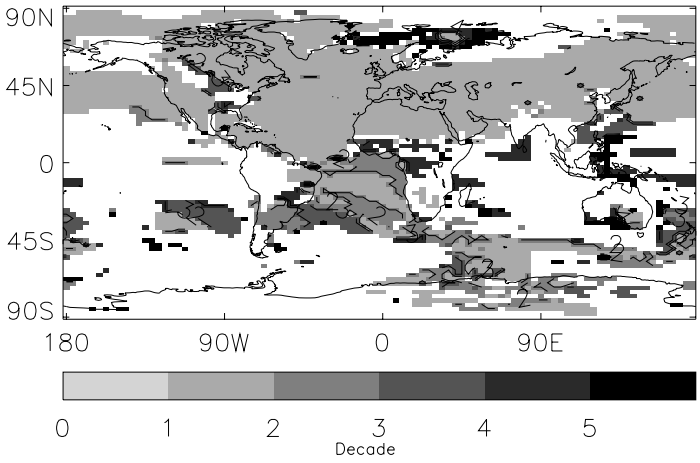

Figure 1: Spread of surface air temperature anomalies. The shading indicates the first decade in which a significant anomaly has persisted for two or more decades.

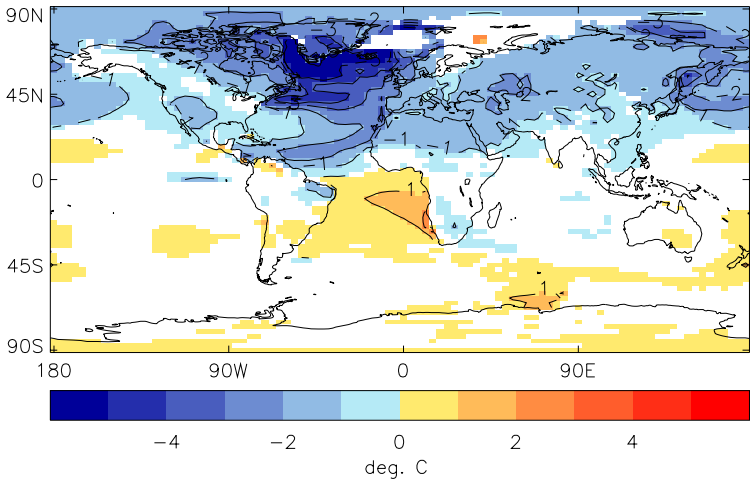

Figure 2: Change in surface air temperature during years 20-30 after the collapse of the THC.. Areas where the anomaly is not significant have been masked.

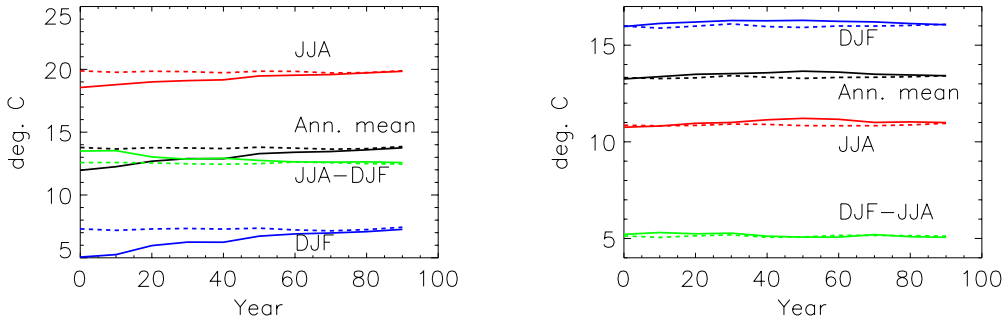

(a) Northern Hemisphere

(b) Southern Hemisphere

Figure 3: Average surface air temperature (in ^oC) in (a): the Northern Hemisphere (b): Southern Hemisphere. The solid lines show evolution of temperature in the perturbation run, the dashed lines show the same quantities for the unperturbed control climate. Blue, red and black show decadally averaged DJF, JJA and annual means, resp. The green curves show the amplitude of the seasonal cycle.

Okhotsk is caused by increased sea-ice cover (Vellinga and Wood (2001)) that isolates the atmosphere from the relatively warm sea surface and augments the cooling. The atmospheric circulation effectively spreads the signal over large parts of the Northern Hemisphere. This results in significant cooling up to 2^oC over Asia and North America.

The Northern Hemisphere cooling occurs in both the boreal winter ('DJF') and summer ('JJA') months, but the effect is stronger in winter (Figure 3a). This inequality increases the amplitude of the seasonal cycle of the Northern Hemisphere by up to 1^oC. The areas with the strongest seasonal component in the temperature response are the Northwestern Atlantic and Labrador Sea and the Sea of Japan and Sea of Okhotsk. As mentioned before, these areas are covered by an anomalously large amount of sea ice. The sea ice cover is particularly extensive in DJF, a time of year when sea ice cover has a large control on surface air temperature. The anomalous sea ice cover melts during JJA, which allows for heat exchange between ocean and atmosphere, and abates the cooling.

The Central England Temperature ('CET') dataset provides a continuous daily temperature record representative of central England for 1772-1991 (Parker *et al.*

(1992)), with monthly mean temperatures going back to 1659 (Manley (1974)). To put the 3^oC cooling of western Europe (Figure 2) into perspective it is worth pointing out that in the entire observed CET record prolonged cooling (two decades with cooling of around $1\,^oC$ relative to 1961-1990 normals) occurs only once, at the end of the 17th century.

In the first decade of the perturbation experiment the (model equivalent of) daily maximum CET is on average four degrees cooler than the normals of the control experiment. (Figure 4a). During spring and autumn average maximum temperatures are colder than the coldest 5% of days that occur in the control experiment.

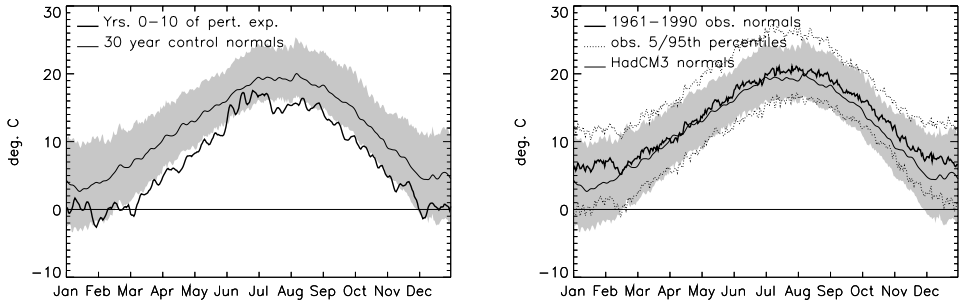

(a) Perturbed climate

(b) Control climate

Figure 4: (a): Daily maximum temperature in central England in HadCM3. The thin curve shows normals for 30 years of the control run (taken from the period parallel to the perturbation experiment); its 5th and 95th percentile values are indicated by the shading. Smoothed values averaged over years 1-10 after THC collapse are shown by the heavy solid line. (b): Thin line and shading as in (a); the heavy solid line shows the observed maximum daily CET normals (Parker et al. 1992), the dotted line its 5th and 95th percentile values.

One has to treat the model CET data with some care as HadCM3 has a cold bias relative to observed values of 1961-1990 (Figure 4b). In the model normals are colder than observed (1.4^oC for the annual mean, 2^oC in DJF). The bias could point to a systematic model error in the model average although the model's maximum CET data are well covered by 90% of the most commonly *observed* values between 1961-1990.

While the Northern Hemisphere cools the Southern Hemisphere warms, slightly; the average temperature rises by a few tenths of a degree (Figure 3b). Warming is strongest over the South Atlantic, up to 1^oC. Elsewhere there is a patchy pattern of warm anomalies emerging from the natural variability. It takes about 40 years before the maximum warming sets in, indicating slow adjustment of the oceans and atmospheric radiation budget. There is, however, a 'fast' route by which warm sea surface temperature anomalies leave the South Atlantic and rapidly propagate eastward on the Antarctic Circumpolar Current in the Southern Ocean (Figure 1). The Northern Hemisphere cooling and Southern Hemisphere warming persist for about 80 years.

The pattern and magnitude of Northern Hemisphere cooling of Figure 2 is comparable to that described by Manabe and Stouffer (1997), who forced a collapse of the THC in the GFDL climate model. The area of maximum cooling in their experiment is shifted to the east, but also shows widespread Northern Hemisphere cooling of about 1^oC. Schiller *et al.* (1997) quote values for maximum cooling of over 15^oC for the annual mean. Apparently the strong cooling in their model is caused by extensive growth of sea ice, partly created by the flux adjustment of heat. Weak Southern Hemisphere warming is a common response in all of these experiments (Schiller *et al.* (1997); Manabe and Stouffer (1997)).

3.2 Surface pressure and winds

The temperature response in the atmosphere extends from the surface to the stratosphere, thereby changing the geopotential height field and general circulation of the atmosphere. We limit the discussion here to changes at $1000\,hPa$. Exact positioning and other details of the anomaly pattern vary from decade to decade but the main features are robust during the first 100 years of the experiment. In the extratropics the response has a distinct seasonal component (Figure 5). In DJF the most important features are positive height anomalies over the North Atlantic and Europe, and negative height anomalies over the Greenland Sea and near the Aleutians. In the extratropics the velocity response is more or less geostrophic, giving enhanced westerlies in western Europe and the North Pacific of $1-2\,m/s$ for the seasonal mean. In the tropical Atlantic height anomalies drive an anomalous southward, cross-equatorial flow. This is related to an enhanced rising branch of the Hadley circulation during DJF and a southward shift of the ITCZ (Vellinga and Wood (2001)). The anomalous equatorial flow persists during JJA, but elsewhere in the Atlantic anomalies are weak. Significant changes are now prevalent in the Southern Ocean and the North Pacific.

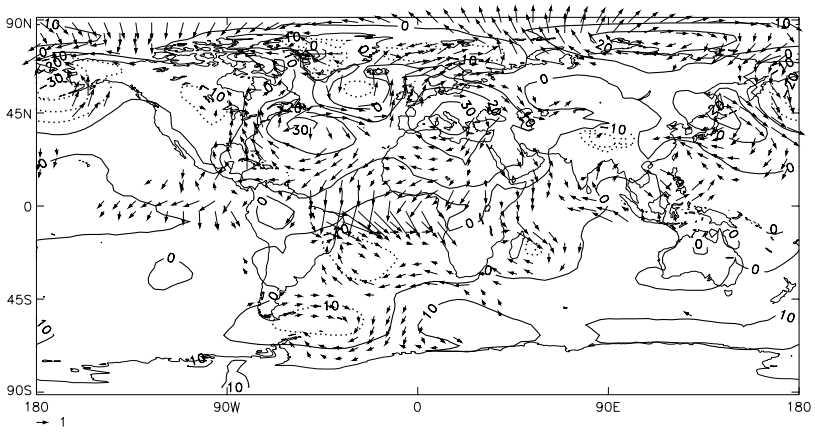

a. DJF anomalies

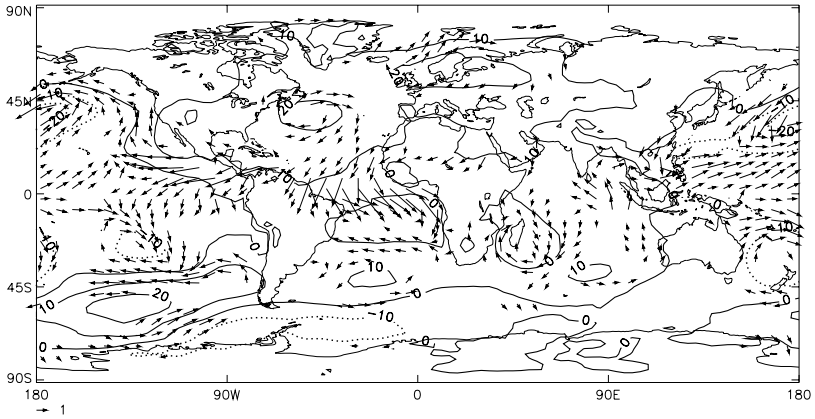

b. JJA anomalies

Figure 5: $1000\,hPa$ height anomalies in m (contours) and significant velocity anomalies in m/s (arrows) for years 20-30 after the collapse of the THC. (a) Anomalies for DJF. (b) Anomalies for JJA

To our knowledge there exist no relevant published results elsewhere to compare these changes to. Manabe and Stouffer (1988) report higher mean sea level pressure where cooling occurs in a climate without a THC (eg. in the North Atlantic). The absence of a seasonal cycle in the solar radiation in their experiment makes a comparison difficult, as we have identified the prominence of seasonal variations in the response.

3.3 Precipitation and evaporation

In contrast with the clear-cut north-south division of surface air temperature anomalies the response in precipitation exhibits a large spatial variation. The areas that experience the largest changes are the tropical Atlantic and the tropical Pacific, Figure 6a. This is a result from the southward shift of the ITCZ (section 3.2). Precipitation anomalies associated with this shift are on the order of $0.8 - 1\, m/year$. A comparable response was reported by Schiller *et al.* (1997) and Manabe and Stouffer (1988). Rainfall in the Northern Hemisphere midlatitudes is reduced, consistent with the cooling: less water vapour can be held by colder air. Although the total amount of precipitation in Europe is reduced by about $0 - 0.2\, m/\, year$ some of the high ground (Scotland, Norway, the Alps) receives significantly more snowfall ($20 - 30\ cm/\, year$). Snow cover in northwest and central Europe lasts on average 1-2 months longer each year in the first decade after the THC collapse.

For a few areas Figure 8 illustrates the magnitude of precipitation anomalies, as well as their duration in summer and winter seasons. The reduction in precipitation in western Europe after the THC collapse is the same in both seasons (Figure 8a,b). In certain parts of the tropics the seasonal migration of the ITCZ creates a large seasonal cycle of rainfall. The changed positioning of the ITCZ due to the collapse of the THC introduces a seasonal component in the climate response; e.g. in eastern Brazil (Figure 8c,d) the wet season becomes significantly wetter, with little (absolute) change of rainfall in the dry season. During DJF the area of the tropical South Atlantic still receives more precipitation than under normal conditions. But unlike in JJA most of this falls over the ocean, and in DJF misses continental South America. Conversely, rainfall in Venezuela and central America is reduced by $1 - 1.5\, mm/day$ in the first 50 years, a reduction of 30% in JJA and 50% in DJF. Over the Indian subcontinent (Figure 8e,f), DJF rainfall shows a decline that is typical for the Northern Hemisphere, caused by the cooling effect. But during JJA the southwest monsoon weakens (as measured by $850\, hPa$ winds, not shown) which results in a stronger reduction of precipitation.

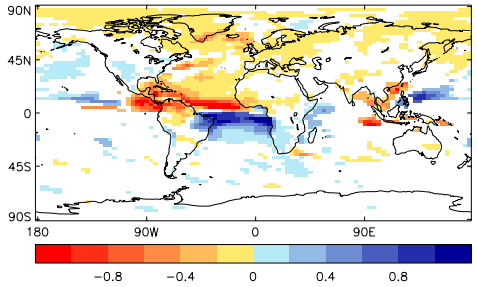

(a) Precipitation

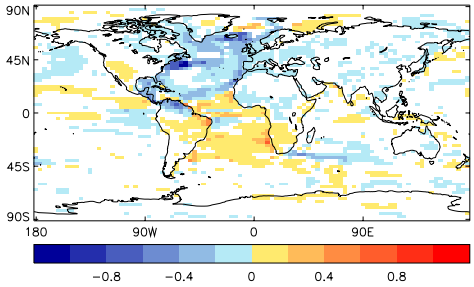

(b) Evaporation

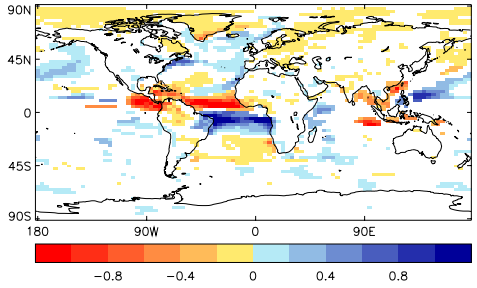

(c) Precipitation minus evaporation

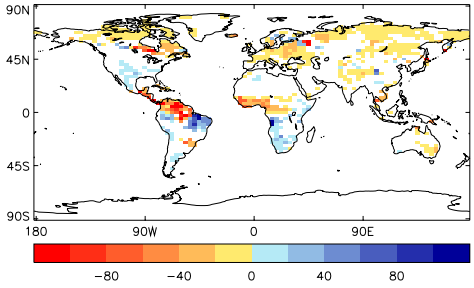

(d) Soil moisture

Figure 6: Significant changes during years 20-30 of the experiment of annual mean (a) precipitation (b) evaporation into the atmospheric boundary layer (c) precipitation surplus (d) soil moisture available to vegetation. Units are $m\,year^{-1}$ ((a)–(c)) and $kg\,m^{-2}$ (d). Blue (red) colours indicate anomalously wet (dry) conditions.

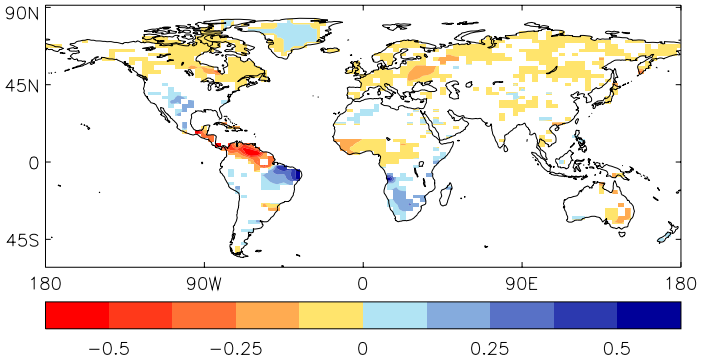

Figure 7: Significant change in net primary production in $kg\,\mathrm{carbon}\,m^{-2}\,year^{-1}$, in years 20-30 after THC collapse.

Evaporation changes (Figure 6b) reflect the north-south pattern of cooling-warming of surface air temperature and partly offsets the precipitation anomalies, notably over the North Atlantic Ocean. By and large the net effect (Figure 6c) is, however, dominated by precipitation.

The change in the amount of soil moisture of the land surface (Figure 6d) follows the change in precipitation minus evaporation. Eastern South America, southern Africa and Mexico are areas with increased soil moisture content. But drier soil conditions elsewhere (Venezuela, Upper Guinea and large parts of Europe, Asia and North America) dominate. During the Younger-Dryas (11,500 years BP), a period of sudden cooling, after a period of deglaciation that is associated with a weakening of the THC, it is believed that drier conditions than modern are believed to have existed worldwide (Alley and Clark (1999)).

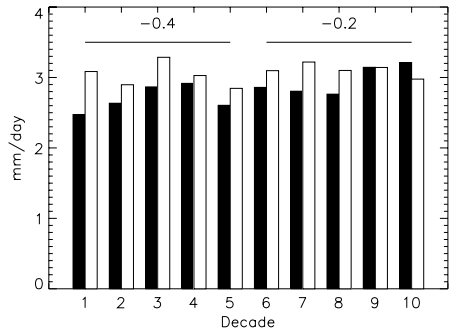

(a) DJF western Europe

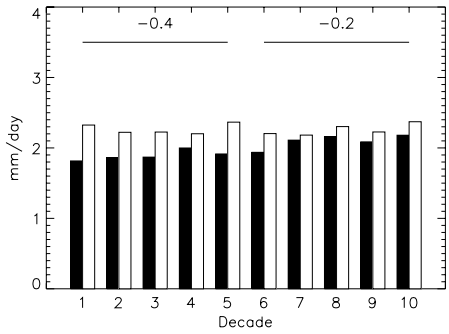

(b) JJA western Europe

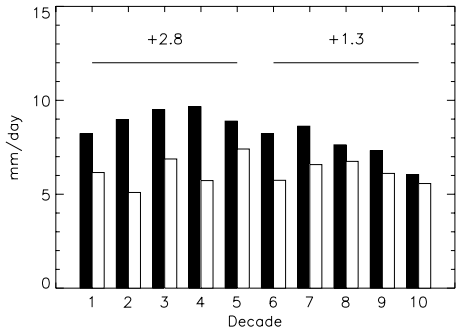

(c) DJF north eastern Brasil

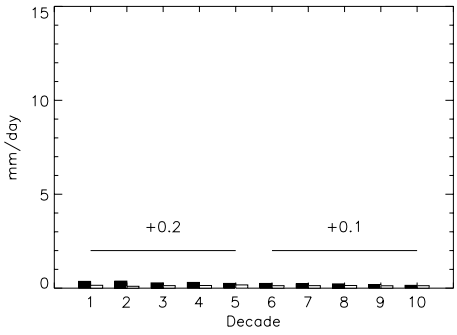

(d) JJA north eastern Brasil

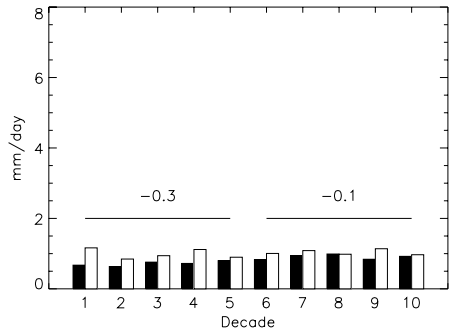

(e) DJF Indian subcontinent

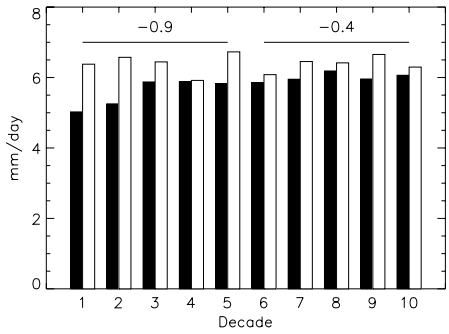

(f) JJA Indian Subcontinent

Figure 8: Average rainfall in mm/day for the perturbed climate (black bars) and the control climate (white bars). Average anomalies during the first and last 50 years of the perturbed climate are given.

3.4 Vegetation net primary production

In addition to the ocean, atmosphere and sea-ice components HadCM3 also includes a land surface scheme (Cox *et al.* (1999)). It defines geographically varying surface parameters, including contributions from 23 types of vegetation, that are averaged over each grid box. The fractional area of the vegetation types are geographically variable but constant in time.

Output from the land surface scheme includes soil moisture, and primary productivity and respiration of CO_2 by the terrestrial vegetation. These latter fields are purely diagnostic in HadCM3 since it does not include a carbon cycle. The difference between gross primary productivity and respiration is net primary productivity, a measure of the yield or harvest of the vegetation. It depends on factors such as soil moisture content, air temperature and incoming shortwave radiation. In a coupled climate-carbon cycle model (Cox *et al.* (2000)) a steady state would be achieved when carbon fluxes due to mortality and net primary productivity balance.

	Control mean	Standard dev.	Pert. mean	Anomaly
Australia	3.5	0.2	3.2	-0.3
Asia	12.3	0.1	11.2	**-1.2**
Indian Subcontinent	0.90	0.07	0.57	**-0.32**
Europe	5.5	0.1	4.6	**-0.9**
Africa	8.4	0.3	8.4	0
North America	8.4	0.2	8.6	+0.1
Central America	0.34	0.08	-0.03	**-0.37**
South America	11.5	0.3	11.4	-0.1
NH	35.1	0.4	31.3	**-3.8**
SH	17.2	0.5	18.2	**+1.1**
Globe	52.2	0.7	49.5	**-2.8**

Table 1: Net primary productivity by the vegetation, integrated over the respective continental landmasses, in Gton carbon per year. Shown are the mean values and standard deviations for the control experiment (first two columns), the mean for the first 30 years of the perturbation experiment (third column), and the anomaly during the first 30 years, with significant anomalies in bold (fourth column). Negative productivity means the vegetation cannot be sustained and would die in a fully interactive vegetation scheme.

The response in net primary production of the vegetation to the climate perturbation reflects the changed atmospheric conditions (Figure 7). The colder and drier conditions over Eurasia cause reductions of order $\mathcal{O}(10\%)$ here (Table 1). Central-America is particularly strongly affected, due to the lower rainfall. In Africa, North and South America the large regional differences cancel out in the totals (cf. shift of ITCZ and the rainfall over South America; wetter conditions in southern North America, colder and drier in the north). The global integral shows a reduction of about $3\,\mathrm{Gton\,C/year}$. In a climate model with active vegetation and carbon components, a fraction of the vegetation would have died as a result and some of the associated carbon would have been released to the atmosphere as CO_2, introducing a feedback between THC and carbon cycle.

The oceanic carbon cycle is sensitive to changes in SST (which affects carbon solubility), to the amount of sea ice cover, and to the amount of vertical mixing and deep water formation that ventilates the deep ocean, (e.g. Sarmiento *et al.* (1998)). To determine how significant the changes in the terrestrial carbon cycle from Table 1 are, compared to those that a THC collapse would cause to the oceanic carbon cycle, requires a study with a coupled climate carbon-cycle model (Cox *et al.* (2000)).

4 Conclusions

We analysed the climate response in HadCM3, a state of the art climate model without flux adjustments, after the Atlantic thermohaline circulation ('THC') was suppressed by a large, instantaneous input of freshwater into the North Atlantic. Other experiments with HadCM3 do not predict a collapse of the THC in the next century under realistic scenarios (Wood *et al.* (1999); Thorpe *et al.* (2001)). But processes controling the stability of the THC—in models and in the real world—are currently not completely understood, and the response that we have described provides an upper bound on the uncertainty in climate predictions that could be caused by incorrectly modelling the stability of the THC. Furthermore, the magnitude, duration and spreading of climatic anomalies could be used in studies of the impacts that a THC collapse would have. No attempt has been made here to estimate the likelihood of such an event.

Temperature response is strongest around the North Atlantic, but covers large parts of the globe within two decades. In the first 50 years strong cooling in the Northern Hemisphere ($1 - 2^oC$) is only partly offset by weak warming in the Southern Hemisphere ($0 - 0.5^oC$). Regional cooling over Europe and eastern

North America is $2 - 3^oC$, with maximum cooling of 8^oC over the northwest Atlantic.

Significant changes in the global distributions of surface winds, rainfall, evaporation and soil moisture stress the active role that the THC plays in shaping global climate. Results also suggest that a THC collapse could lead to a global reduction in net primary production by the terrestrial vegetation of about 5%. The model used here does not include carbon cycle feedbacks and one must treat this finding with caution.

The predicted global warming over the next century due to rising greenhouse gas and aerosol concentrations is estimated to lie between $1 - 3.5^oC$ (Houghton *et al.* (1996)). The global temperature change due to the collapse of the Atlantic THC varies from -1^oC in the first decade to about -0.3^oC in years 40-50 (Vellinga and Wood (2001)). Local temperature change after the THC collapse can be much stronger than this. In a simple linear superposition the cooling due to a hypothetical THC collapse in, say 2050, would outweigh the warming due to increased greenhouse gas concentrations around the North Atlantic in this model.

This study highlights the need to reduce the uncertainties in our climate models regarding the stability of the THC. An unforeseen or wrongly predicted collapse of the THC would lead to significant errors in global and especially regional climate predictions. Efforts to reduce the uncertainty in modelling the stability of the THC in HadCM3 are ongoing. This starts with the analysis of the dominant physical processes that determine size and nature of the response by the THC when it is subjected to various kinds of stress (Thorpe *et al.* (2001); Vellinga and Wood (2001)). In the next stage one would then attempt to eliminate modelling errors from these same processes.

Note

Additional data from this experiment can be made available on request.

Acknowledgements

We like to thank Peter Cox, Steven Spall, Jonathan Gregory, Howard Cattle and Geoff Jenkins for suggestions and stimulating discussions; Briony Horton for making the CET data available, and Ian Macadam for calculating the model CET data. This work was funded by the Department of the Environment, Transport and Regions under the Climate Prediction Programme PECD/7/12/37.

Bibliography

Alley, R. B. and Clark, P. U. 1999 The deglaciation of the Northern Hemisphere: a global perspective. *Annu. Rev. Earth Planet. Sci.*, **27**, 149–182.

Cox, P. M., Betts, R. A., Bunton, C. B., Essery, R. L. H., Rowntree, P. R., and Smith, J. 1999 The impact of new land surface physics on the GCM simulation of climate and climate sensitivity. *Clim. Dyn.*, **15**, 183–203.

Cox, P., Betts, R., Jones, C., Spall, S., and Totterdell, I. 2000 Acceleration of global warming due to carbon–cycle feedbacks in a coupled climate model. *Nature*, **408**, 184–187.

Gordon, C., Cooper, C., Senior, C. A., Banks, H., Gregory, J. M., Johns, T. C., Mitchell, J. F. B., and Wood, R. A. 2000 The simulation of SST, sea ice extents and ocean heat transports in a version of the Hadley Centre coupled model without flux adjustments. *Clim. Dyn.*, **16**, 147–168.

Gordon, A. L. 1986 Inter-ocean exchange of thermocline water. *J. Geophys. Res.*, **91**, 5037–5046.

Houghton, J. T., Meira Filho, L. G., Callander, B. A., Harris, N., Kattenberg, A., and Maskell, K. 1996 *Climate Change 1995 — The Science of Climate Change*. Cambridge University Press, Cambridge. 572 pp.

Keller, K., Tan., K., Morel, F., and Braidford, D. 2000 Preserving the ocean circulation: implications for climate policy. *Climatic Change*, **47**, 17–43.

Latif, M., Roeckner, E., Mikolajewicz, U., and Voss, R. 2000 Tropical stabilisation of the thermohaline circulation in a greenhouse warming simulation. *J. Climate*, **13**, 1809–1813.

Macdonald, A. M. and Wunsch, C. 1996 An estimate of global ocean circulation and heat fluxes. *Nature*, **382**, 436–4392.

Manabe, S. and Stouffer, R. J.	1988	Two stable equilibria of a coupled ocean-atmosphere model. *J. Climate*, **1**, 841–866.
Manabe, S. and Stouffer, R. J.	1994	Multiple century response of a coupled ocean-atmosphere model to an increase of atmospheric carbon dioxide. *J. Climate*, **7**, 5–23.
Manabe, S. and Stouffer, R. J.	1997	Coupled ocean-atmosphere model response to freshwater input: Comparison to Younger-Dryas event. *Paleoceanography*, **12**, 321–336.
Manabe, S. and Stouffer, R. J.	1999	Are two modes of thermohaline circulation stable? *Tellus*, **51 A**, 400–411.
Manley, G.	1974	Central England temperatures, monthly means 1659 to 1973. *Quart. J. R. Met. Soc.*, **79**, 242–261.
Parker, D. E., Legg, T. P., and Folland, C. K.	1992	A new daily Central England temperature series. *Int. J. Climatol.*, **12**, 317–342.
Pope, V. D., Gallani, M. L., Rowntree, P. R., and Stratton, R. A.	2000	The impact of new physical parametrizations in the Hadley Centre climate model – HadAM3. *Climate Dyn.*, **16**, 123–146.
Sarmiento, J., Hughes, T., Stouffer, R., and Manabe, S.	1998	Simulated response of the ocean carbon cycle to anthropogenic climate warming. *Nature*, **393**(6682), 245–249.
Sarnthein, M., Winn, K., A.Jung, S. J., Duplessy, J. C., Labeyrie, L., and et al	1994	Changes in east Atlantic deep water circulation over the last 30,000 years: eight time slice reconstructions. *Paleoceanography*, **9**, 209–267.
Schiller, A., Mikolajewicz, U., and Voss, R.	1997	The stability of the thermohaline circulation in a coupled ocean-atmosphere general circulation model. *Clim. Dyn.*, **13**, 325–347.

Thorpe, R., J.M.Gregory, T.C.Johns, and J.F.B.Mitchell 2001 Mechanisms underpinning the response of the thermohaline circulation to greenhouse gas forcing in a non-fluxadjusted coupled climate model. *acc. J. Climate*.

Vellinga, M. and Wood, R. 2001 Climate response to a suppression of the Atlantic thermohaline circulation. *Subm. J.Climate*.

Wood, R. A., Keen, A. B., Mitchell, J. F. B., and Gregory, J. M. 1999 Changing spatial structure of the thermohaline circulation in response to atmospheric CO_2 forcing in a climate model. *Nature*, **399**, 572–575.